Journal of Hazardous Materials, 16 (1987) 231–245
Elsevier Science Publishers B.V., Amsterdam — Printed in The Netherlands

FIELD TEST VALIDATION OF THE DEGADIS MODEL

T.O. SPICER and J.A. HAVENS
Department of Chemical Engineering, University of Arkansas, Fayetteville, AR 72701 (U.S.A.)
Received November 13, 1986; accepted February 22, 1987)

Summary

An interactive computer model (DEGADIS) which uses a lumped parameter approach to simulate a wide variety of denser-than-air gas release scenarios, including instantaneous releases, time-varying releases, and continuous releases on a flat, obstacle-free surface is briefly described. The model accounts for negative buoyancy-induced and stably stratified shear flows and is consistent with the limiting passive dispersion characteristics of demonstrated air pollution models.

Predicted maximum concentration as a function of distance is compared to the maximum reported concentration for field scale releases of liquefied natural gas (LNG), liquefied petroleum gas (LPG as propane), and Freon-12/nitrogen mixtures from the Burro/Coyote, Maplin Sands, and Thorney Island Phase I trials, respectively. From these, the variability of the distance realized to a concentration level of 5, 2.5, and 1% for a given release is quantified based on the predicted distance. Comparisons of observed and model-predicted dispersion of nitrogen tetroxide from a large scale field test program (the U.S. Air Force Eagle series) are also presented.

1. Introduction

Consider a ground-level release of a mass of denser-than-air gas (DTAG) on flat, obstacle-free terrain. The initial gas cloud may result directly from (1) an aboveground release such as a release of pressurized gases, as in a chlorine tank rupture, or (2) indirectly from a ground-level source such as the evaporation of a released liquid as in the case of a spill onto the sea of liquefied petroleum gas (LPG) or natural gas (LNG). The cloud may be initially formed as a mixture of gas or gas–liquid aerosol and (humid) air. In general, such a release would be expected to pass through three phases: (1) negative buoyancy-dominated dispersion, (2) passive dispersion, and (3) stably stratified shear flow.

1.1 Negative buoyancy-dominated dispersion phase

Rapid release of a DTAG may result in an initial cloud having similar vertical and horizontal dimensions. The initial behavior of such "compact clouds" [1] is controlled by the negative buoyancy-driven flow. The gravity-driven flow results in large scale turbulent structures which cause the cloud to dilute

0304-3894/87/$03.50

[2–6]. Since this initial turbulent motion can result in dilution by a factor larger than ten, it must be accounted for in predictions of DTAG dispersion, particularly for hydrocarbons. (Gas–air mixture flammability levels for hydrocarbons are generally O (1%).)

1.2 Passive dispersion phase

At some distance from the source, the released gas will be sufficiently dilute to justify its consideration as a trace material, and the dispersion can be modeled using approaches developed for atmospheric pollutant dispersion [7,8]. The Gaussian plume model is applicable to atmospheric dispersion problems when the dispersion of the contaminant is only a function of the atmospheric turbulence and the plume does not perturb the ambient flow field. The steady-state Gaussian plume model for ground-level releases is

$$y_v = \frac{Q}{\pi \sigma_y \sigma_z u} \exp\left[-\left(\frac{y}{\sqrt{2}\,\sigma_y}\right)^2 - \left(\frac{z}{\sqrt{2}\,\sigma_z}\right)^2 \right] \tag{1}$$

where σ_y and σ_z determine the shape of the Gaussian profile. Prescriptions for σ_y and σ_z as a function of distance are given by Hanna et al. [7] and Pasquill and Smith [8].

1.3 Stably stratified shear flow phase

The distinguishing feature of a neutrally buoyant plume described above is the assumption that the mean flow field is not affected by the contaminant. This is in direct contrast to the negative buoyancy-dominated flow phase where the distinguishing feature is the essentially complete determination of the mean flow field by the contaminant release as described above. An intermediate phase of the dispersion process is characterized by its similarity to a wide variety of naturally occurring flow processes in which a stably stratified plume is embedded in a turbulent mean flow. Such plumes are expected to differ importantly from neutrally buoyant plumes.

1. A lateral (crosswind) gravity-driven mean flow will persist until the negative buoyancy of the cloud has been reduced (by air entrainment).
2. Because the ratio of width to depth for these plumes is characteristically large, dilution occurs primarily as a result of vertical mixing.
3. The density stratification at the upper plume boundary should act to damp turbulent mixing and consequently reduce vertical mixing (air entrainment).

Fluid mixing across the density interface which characterizes a dense plume embedded in a turbulent boundary layer was reviewed by Turner [9]. There is general agreement that entrainment across such plume boundaries is correlated with a bulk Richardson number ($Ri_* = g\Delta' H/u_*^2$). McQuaid [10], Kantha et al. [11], and Lofquist [12] have reported experimental studies from

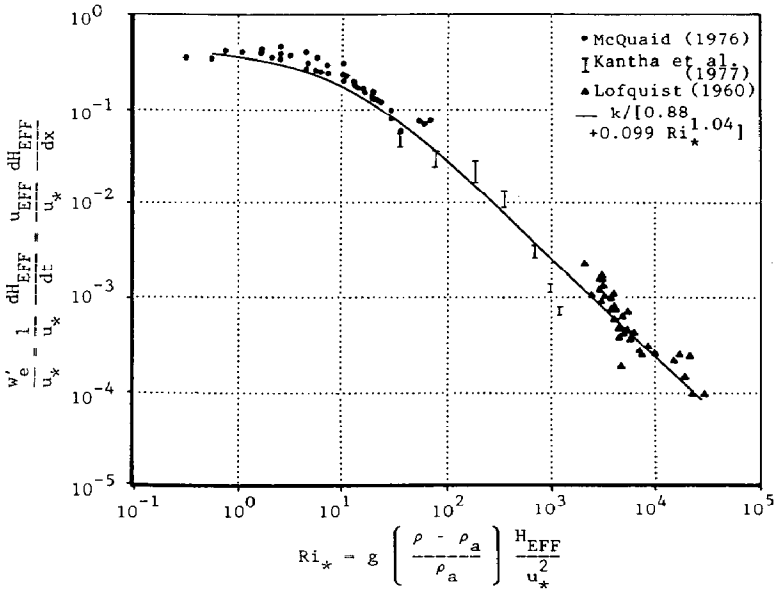

Fig. 1. Correlation of entrainment velocity with bulk Richardson number.

which entrainment velocity correlations can be derived for Richardson numbers encompassing the range of interest for DTAG dispersion.

The combined data of McQuaid, Kantha et al., and Lofquist shown in Fig. 1 were curve-fitted to give

$$w'_e/u_* = k/(0.88 + 0.099\, Ri_*^{1.04}) \tag{2}$$

The limiting value ($Ri_* = 0$) of $w'_e/u_* = k/0.88$ incorporates the ratio of eddy diffusivities for heat and momentum (K_H/K_M), along with $k = 0.35$ (as determined by Businger et al. [13] from measurements in the neutral atmospheric surface stress layer). The effect of vertical density stratification on vertical mixing shown by the data is consistent with a passive limit for w'_e/u_* of 0.4 as suggested by the solution of the diffusion equation with a constant wind velocity and mass diffusivity given by

$$K_c = k u_* z \tag{3}$$

(which is consistent with the Gaussian plume model of eqn. 1). Furthermore, the dependence of w'_e on Ri_* for large Ri_* approaches

$$w'_e \propto Ri_*^{-1} \tag{4}$$

as suggested from dimensional reasoning by Turner [9].

2. The DEGADIS model

DEGADIS [14] is an adaptation of the Shell HEGADAS model described by Colenbrander [15] and Colenbrander and Puttock [16]; DEGADIS also incorporates some techniques used by van Ulden [17]. The near-field, buoyancy-dominated regime is modeled using a lumped parameter model of a DTAG "secondary source" cloud which incorporates air entrainment at the gravity-spreading front using a frontal entrainment velocity. The downwind dispersion phase assumes a power law concentration distribution in the vertical direction and a modified Gaussian profile in the horizontal direction with a power law specification for the wind profile (Fig. 2). The source model represents a spatially averaged concentration of gas present over the primary source, while the downwind dispersion phase of the calculation models an ensemble average of the concentration downwind of the source.

For the negative buoyancy-dominated dispersion phase, the model is based on laboratory-scale releases of a DTAG in a calm environment [5,6]. For the stably stratified shear flow phase, the model is based on the laboratory-scale experiments of McQuaid [10], Kantha et al. [11] and Lofquist [12] discussed in Section 1.3. Established passive atmospheric dispersion modeling principles are used for the passive dispersion phase. It is emphasized that DEGADIS was not calibrated to any DTAG field-scale tests. A complete description of the DEGADIS model is included in Havens and Spicer [14].

3. Analysis and simulation of selected field experiments

The DEGADIS model has been used to simulate a large collection of field experimental DTAG releases (Table 1). The field tests simulated include small continuous LPG releases (order 0.1 to 1.0 kg/s) on land from diked sources, continuous LPG and LNG releases onto water with release rates of the order 10–100 kg/s, instantaneous releases of LNG onto water of approximately 5000 kg, instantaneous releases of Freon-12/nitrogen mixtures of approximately 5000 kg on land, and quasi-steady releases of nitrogen tetroxide (N_2O_4). The meteorological conditions in the experimental releases include wind speeds of approximately 1.0–10.0 m/s, relative humidity from essentially zero to about 85%, and atmospheric stabilities ranging from Pasquill B to E. In general, the field tests of Table 1 were directed toward either hydrocarbon flammability levels (O(1%)) or toxic gas levels (O(100 ppm)). (A complete summary of simulated releases can be found in Havens and Spicer [14] and Spicer and Havens [18].)

3.1 Hydrocarbon flammability levels — O(1%)

All of the field scale experimental programs in Table 1 except the USAF Eagle series were directed to measuring concentrations no lower than O(0.1%).

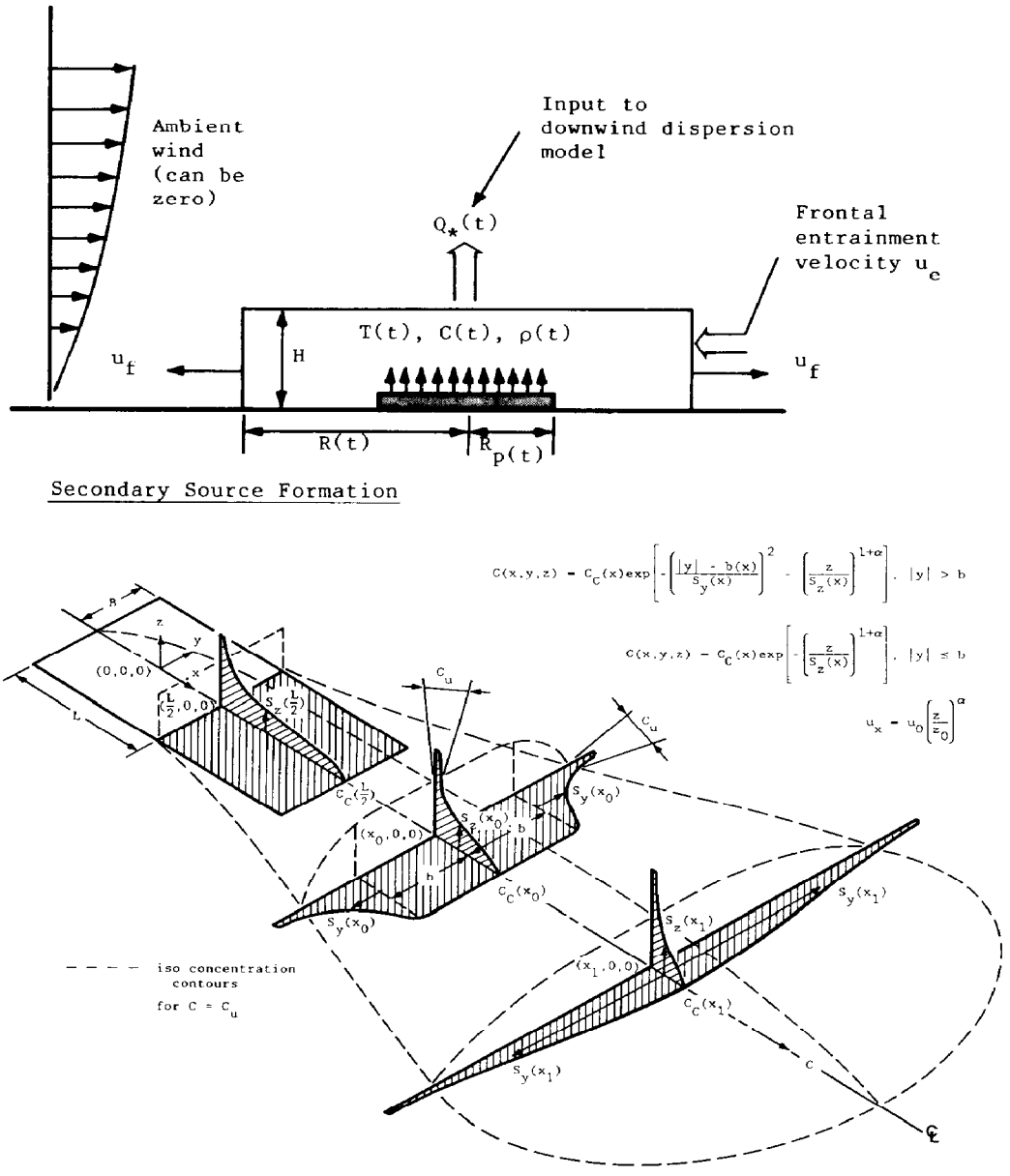

Fig. 2. Schematic diagram of DEGADIS denser-than-air gas dispersion model.

In the U.S. DOE releases reported by Welker [19], propane was released into concrete-lined pits nominally 1.5, 3, and 6 meters square. Peak (or maximum reported) and mean concentrations were reported at ground level at positions estimated to be in the plume centerline. Figure 3 is a typical compar-

TABLE 1

Summary of field experimental DTAG releases

Test series	Material released	Release type/size	Wind speed range (m/s)	Pasquill stability range	Release Richardson number[a]
British Health & Safety Executive, Thorney Island	Freon-12/ nitrogen mixtures	Instantaneous, 3500–4800 kg	1.7–7.5	C–E	—
Shell Research, Maplin Sands	LNG and LPG[b]	Steady state, 17.7–41.7 kg/s	4.1–9.8	D	4–100
USAF Eagle series releases	Nitrogen tetroxide	Steady state, 1.6–3.0 kg/s	3.7–5.6	D	4–40
U.S. DOE Burro, Coyote series releases	LNG and LPG[b]	Continuous, time-limited, $9.7\text{–}16.7\times10^3$ kg	2.4–11.9	C–E	4.7–930
U.S. DOE releases by Welker	LPG[b]	Steady state, 0.019–0.55 kg/s	2.0–7.5	B–D	0.1–3.5

[a]The continuous release Richardson number is defined by

$$Ri_c = \frac{g}{u_*^2}\left[\frac{\rho_i - \rho_a}{\rho_a}\right]\left[\frac{\dot{m}}{\rho_i u D}\right]$$

where $\dot{m}$ is the contaminant evolution rate (kg/s), u is the ambient wind velocity (m/s) specified at an (arbitrary) height, and D is the source diameter. Ri_c represents a ratio of the potential energy characteristic of the release to a measure of the ambient turbulent kinetic energy. Three ranges of Ri_c are important: $Ri_c < 1$ release is passive from the source; $1 \leqslant Ri_c \leqslant 32$ release is in the stably stratified shear flow phase; $Ri_c > 32$ release is in the negative buoyancy-dominated dispersion phase. The Thorney Island trials release Richardson numbers were not calculated since these are instantaneous releases.

[b]LPG was predominantly propane.

ison of the reported centerline concentrations to the DEGADIS-predicted maximum centerline concentration. Welker showed the reported centerline concentrations to be described reasonably well by a passive dispersion model in agreement with the release Richardson number range in Table 1.

In contrast to the small release Richardson numbers of the releases reported by Welker, the British Helath and Safety Executive releases at Thorney Island were instantaneous releases of nominal 2000 m^3 volumes of Freon-12/nitrogen mixtures [20]. Figure 4 is a typical comparison of the maximum reported concentration to the DEGADIS-predicted maximum centerline concentration.

The U.S. DOE Burro and Coyote series releases were performed by Law-

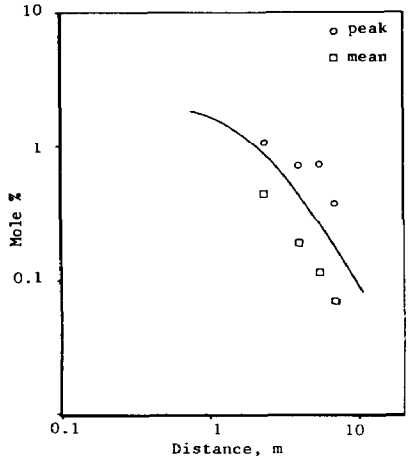

TEST: Welker 275-1

Source Description

Type: Continuous Propane		
Primary Source Width	:	1.52
Secondary Source Width (m)	:	1.52
Primary Source Flux (kg/m^2 s)	:	8.13 E-3
Rate (kg/s)	:	0.0188
Temperature (K)	:	231.0

Meteorological Conditions

Wind Velocity (m/s)	:	4.52
@ Height (m)	:	2.44
Surface Roughness (m)	:	0.01
Pasquill Stability	:	B
Monin-Obukhov Length (m)	:	-11.8
Air Temperature (K)	:	301.5
Relative Humidity (%)	:	28
Surface Temperature (K)	:	305

Release Richardson Number

Volumetric Release Rate (m^3/s)	:	7.88 E-3
Characteristic Width (m)	:	1.52
Estimated Friction Velocity (m/s)	:	0.31

$$Ri_0^C = g\left[\frac{\rho_i - \rho_a}{\rho_a}\right]\frac{Q}{uu_*^2 D} = 0.12$$

Fig. 3. DEGADIS-predicted centerline maximum concentration and reported concentration vs. distance — Welker 275-1.

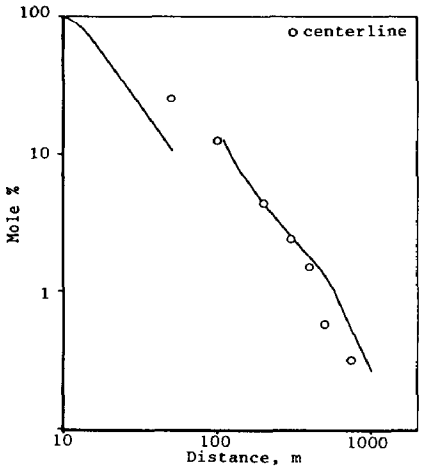

TEST: Thorney 15

Source Description

Type: Instantaneous		
Volume (m^3)	:	2100
Initial Relative Density	:	1.41
Temperature (K)	:	Isothermal

Meteorological Conditions

Wind Velocity (m/s)	:	5.40
@ Height (m)	:	10.0
Surface Roughness (m)	:	1.0 E-2
Pasquill Stability	:	D
Monin-Obukhov Length (m)	:	∞
Air Temperature (K)	:	283.45
Relative Humidity (%)	:	88

Release Richardson Number

Estimated Friction Velocity (m/s): 0.27

$$Ri_0^I = g\left[\frac{\rho_i - \rho_a}{\rho_a}\right]\frac{V_i^{1/3}}{u_*^2} = 690$$

Fig. 4. DEGADIS-predicted centerline maximum concentration and maximum reported concentration vs. distance — Thorney 15.

rence Livermore National Laboratories (LLNL) at China Lake, California [21]. LNG was released on water with subsequent dispersion over land. Figure 5 shows a typical comparison of the DEGADIS-predicted maximum centerline

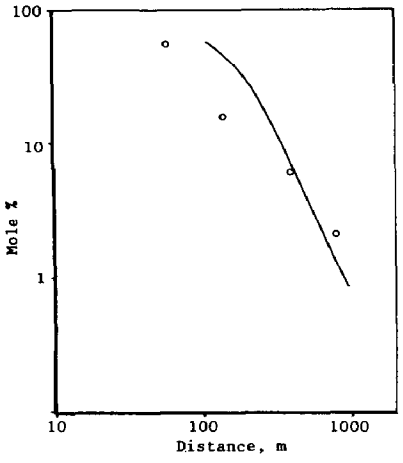

TEST: Burro 8

Source Description

Type: Steady, Time-Limited LNG		
Primary Source Radius (m)	:	20.6
Primary Source Flux (kg/m^2 s)	:	0.085
Rate (kg/s)	:	113.3 for 106 s
Temperature (K)	:	112

Meteorological Conditions

Wind Velocity (m/s)	:	2.4
@ Height (m)	:	8.0
Surface Roughness (m)	:	2.05 E-4
Pasquill Stability	:	E
Monin-Obukhov Length (m)	:	16.5
Air Temperature (K)	:	306.15
Relative Humidity (%)	:	5
Surface Temperature (K)	:	310.0

Release Richardson Number

Volumetric Release Rate (m^3/s)	:	63.2
Characteristic Width (m)	:	36.5
Estimated Friction Velocity (m/s)	:	0.065

$$Ri_0^C = g\left[\frac{\rho_i - \rho_a}{\rho_a}\right]\frac{Q}{uu_*^2 D} = 930.$$

Fig. 5. DEGADIS-predicted centerline maximum concentration and maximum reported concentration vs. distance — Burro 8.

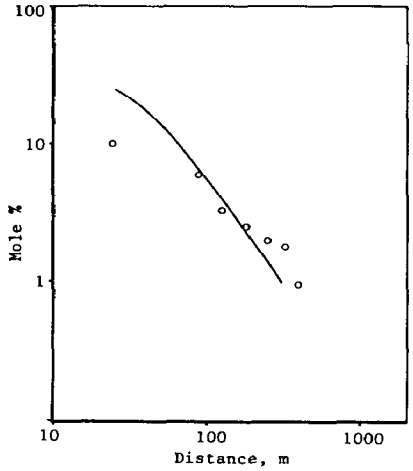

TEST: Maplin 46

Source Description

Type: Continuous Propane		
Primary Source Radius (m)	:	8.49
Primary Source Flux (kg/m^2 s)	:	0.12
Rate (kg/s)	:	27.16
Temperature (K)	:	231.0

Meteorological Conditions

Wind Velocity (m/s)	:	8.1
@ Height (m)	:	10.0
Surface Roughness (m)	:	3.38 E-4
Pasquill Stability	:	D
Monin-Obukhov Length (m)	:	∞
Air Temperature (K)	:	292
Relative Humidity (%)	:	71
Surface Temperature (K)	:	291

Release Richardson Number

Volumetric Release Rate (m^3/s)	:	11.3
Characteristic Width (m)	:	15.1
Estimated Friction Velocity (m/s)	:	0.28

$$Ri_0^C = g\left[\frac{\rho_i - \rho_a}{\rho_a}\right]\frac{Q}{uu_*^2 D} = 11.9$$

Fig. 6. DEGADIS-predicted centerline maximum concentration and maximum reported concentration vs. distance — Maplin 46.

concentration with the reported maximum concentration. The release Richardson number for these tests indicates the importance of the negative buoyancy-dominated dispersion phase and the stably stratified shear flow phase.

The Shell Research releases at Maplin Sands were a series of LNG and LPG (propane) releases on water [22]. Most of the releases were steady state. Two instantaneous releases each of LNG and LPG were reported. Figure 6 shows a typical comparison of the maximum reported (steady) concentrations to the DEGADIS-predicted maximum centerline concentration. As in the Burro and Coyote tests, the release Richardson number indicates the importance of the negative buoyancy-dominated dispersion phase and the stably stratified shear flow phase.

In order to quantify the uncertainty associated with predicted distances to concentrations of order 1%, predicted and "observed" distances to the 5%, 2.5%, and 1% concentration levels were compared. The "observed" values were determined from maximum reported concentrations for each experiment by drawing a visual best-fit straight line through the reported points in the concentration range of interest; all of the measurements used were made at heights at or below 1 m. The predicted distance to a given concentration level was based on the ground level centerline concentration calculated by DEGADIS; for the concentrations and conditions of interest, the predicted concentration level is essentially constant for heights below 1 m. From these values, a ratio of the "observed" to the predicted distance for each experiment was calculated. For this analysis, the ratio $(\mathrm{OBS/PRE})_y$ is assumed to be independent of the release conditions.

Table 2 includes values of the ratios $(\mathrm{OBS/PRE})_y$ along with 90% confidence intervals for the average of $(\overline{\mathrm{OBS/PRE}})_y$ for each test series and for all of the experiments together. (For instance, the Maplin Sands comparisons indicate the average ratio of the "observed" to the predicted distance to the 2.5% concentration level would be between 0.91 and 1.20 in nine out of ten realizations.) For all of the comparisons in Table 2, the 90% confidence interval for the average ratio of "observed" distance to predicted distance for a given concentration level ranged from 0.73 to 0.96 for the 5% level; for the 2.5% level, a 90% confidence interval for $(\overline{\mathrm{OBS/PRE}})_{2.5}$ ranged from 0.82 to 1.03; for the 1% level, a 90% confidence interval for $(\overline{\mathrm{OBS/PRE}})_1$ ranged from 0.95 to 1.24. The confidence intervals of the ratio $(\overline{\mathrm{OBS/PRE}})_y$ can now be used to predict the range of the average distance to a given concentration level under a given set of release conditions.

3.2 Toxic gas levels — O(100 ppm)

In 1983, Lawrence Livermore National Laboratories (LLNL) conducted a series of nitrogen tetroxide (N_2O_4) releases for the U.S. Air Force at the U.S. DOE Nevada Test Site (NTS). Two of these releases, Eagle 3 and 6, provided sufficient data for comparison and assessment of atmospheric gas dispersion

TABLE 2

Comparison between "observed" and DEGADIS-predicted maximum distance to gas concentrations in the flammable concentration range

	Ratio of "observed" distance to DEGADIS-predicted distance $(\overline{OBS/PRE})_y$ for the concentration level y:		
	$y=5\%$	$y=2.5\%$	$y=1\%$
Thorney Island			
7	1.17	1.12	0.63
8	1.09	0.90	0.66
9	1.00	0.95	1.28
11	0.55	0.61	0.63
13	0.70	0.70	0.70
15	1.05	0.90	0.77
Thorney Island 90% confidence interval	$0.71 \leqslant (\overline{OBS/PRE})_5 \leqslant 1.11$	$0.70 \leqslant (\overline{OBS/PRE})_{2.5} \leqslant 1.02$	$0.64 \leqslant (\overline{OBS/PRE})_1 \leqslant 0.99$
Maplin			
22	0.47	0.64	1.15
27	0.95	1.10	1.46
29	0.89	0.96	1.20
34	1.28	1.38	1.76
35	1.28	1.59	2.61
39	0.46	0.63	1.21
43	0.73	0.84	0.91
46	1.09	1.17	1.33
47	0.77	0.92	1.06
49	1.27	1.35	1.46
50	0.92	0.90	1.26
54	1.12	1.21	1.19
56	0.93	0.92	1.02
Maplin 90% confidence interval	$0.80 \leqslant (\overline{OBS/PRE})_5 \leqslant 1.10$	$0.91 \leqslant (\overline{OBS/PRE})_{2.5} \leqslant 1.20$	$1.15 \leqslant (\overline{OBS/PRE})_1 \leqslant 1.47$
Burro			
3	0.52	0.69	0.83
7	0.63	0.74	0.95
8	0.93	1.21	1.66
9	0.51	0.78	1.22
Coyote			
5	0.75	0.71	0.71
6	0.38	0.38	0.43
Burro/Coyote 90% confidence interval	$0.46 \leqslant (\overline{OBS/PRE})_5 0.78$	$0.55 \leqslant (\overline{OBS/PRE})_{2.5} \leqslant 0.98$	$0.63 \leqslant (\overline{OBS/PRE})_1 \leqslant 1.31$
Summary 90% confidence interval	$0.73 \leqslant (\overline{OBS/PRE})_5 \leqslant 0.96$	$0.82 \leqslant (\overline{OBS/PRE})_{2.5} \leqslant 1.03$	$0.95 \leqslant (\overline{OBS/PRE})_1 \leqslant 1.24$

TABLE 3

Comparison of Eagle 3 and Eagle 6 test results and gas dispersion model predictions [18]

	Maximum NO_2 concentration range (ppm)[a]	σ_y (m)	σ_z (m)
Eagle 3			
Test results	500–1040	35	3.8
Gaussian plume	68–73	60.5	31.9
DEGADIS	880–1170	57.6–60.7[b]	3.2–4.1[c]
Eagle 6			
Test results	160–340	35	7.6
Gaussian plume	25–27	60.5	31.9
DEGADIS	190–220	55.6–56.6[b]	6.4–6.9[c]

[a]The concentration range for the model predictions are for the estimated source mass evolution rate range.
[b]Calculated as $S_y/\sqrt{2}$.
[c]Estimated as S_z.

modeling techniques [23]. An array of sensors designed to measure N_2O_4 concentration, temperature, and velocity was placed 25 m downwind of the gas source to measure the mass evolution rate of the released gas. Another array of sensors designed to measure NO_2 concentration, temperature, and velocity was placed 785 m downwind of the source to measure the concentration of the gas cloud as it moved downwind after release. The Eagle series tests were complicated further by the interaction of N_2O_4 with the ambient humidity which hindered concentration measurements.

Based on the measured N_2O_4 mass rate passing the 25 m sensor array and an analysis of the reactions taking place, Spicer and Havens [18] reported N_2O_4 mass evolution rates between 2.9 and 3.1 kg/s for Eagle 3 and between 1.6 and 1.7 kg/s for Eagle 6 as well as steady-state-observed maximum concentration ranges (expressed as equivalent NO_2 concentration) for Eagle 3 and 6 as summarized in Table 3. Table 3 also includes model predictions from the Gaussian plume model and DEGADIS.

For Eagle 3 and 6, the pasive dispersion model tends to underpredict the maximum concentration because of an overprediction of the vertical mixing rate (i.e. the predicted σ_z is greater than the observed σ_z). On the other hand, DEGADIS predicts maximum centerline concentrations and similarity distribution parameters σ_y and σ_z which are consistent with the experimental data; closer agreement of DEGADIS-predicted values of σ_z with observed values of σ_z compared to the passive Gaussian plume model is attributed to correctly predicting the decreased vertical mixing rate for the initial phase of the releases. These characteristics are consistent with the release Richardson number of each release. ($Ri_c = 40$ for Eagle 3 and $Ri_c = 4$ for Eagle 6.)

Conclusions and recommendations

Based on the phenomenology of DTAG dispersion, the following phases are used to describe DTAG dispersion in the atmosphere:
— Negative buoyancy-dominated dispersion
— Stably stratified shear flow
— Passive dispersion due to atmospheric turbulence
Along with established models for passive dispersion, laboratory experimental data were used to model the other dispersion phases. Laboratory data from stratified shear flow mixing experiments have been used to model the vertical dispersion of DTAG in the atmospheric constant stress layer consistently with the limiting passive dispersion behavior of demonstrated air pollution models. DEGADIS, an interactive computer model for DTAG dispersion, accounts for the three regimes of dispersion described above and for effects due to energy exchange between the dispersing cloud and the underlying surface.

The DEGADIS model has been used to simulate a wide range of field experimental DTAG releases, including small to intermediate LPG (0.1–1 kg/s) and LNG release (1–100 kg/s) on land, large-scale releases (10–150 kg/s) of LPG and LNG on water, instantaneous releases of approximately 5000 kg Freon-/nitrogen mixtures on land, and quasi-steady state releases of N_2O_4 over land. The DEGADIS model-predicted downwind gas concentration decay has been shown consistent with the field-scale experimental data currently available.

Application of DEGADIS has been primarily directed to the prediction of concentrations in the lower flammability limit range (1–5%). Based on comparison with field data, a 90% confidence interval for the average ratio of observed to calculated distance for the 2.5% concentration level would be between 0.82 and 1.03; the 90% confidence interval for the average ratio of observed to calculated distance was between 0.73 and 0.96 for the 5% level and between 0.95 and 1.24 for the 1% level.

Application of DEGADIS to the prediction of concentration levels of interest for toxic gases (O(100 ppm)) for DTAGs is less complete. For Eagle 3 and 6, downwind concentrations and observed Gaussian equivalent concentration profiles (σ_y and σ_z) were compared to model predictions using the Gaussian plume model and DEGADIS. The Gaussian plume model generally underpredicted the concentration due to an overprediction of the vertical mixing present, while DEGADIS predictions were consistent with observed concentrations and profile parameters σ_y and σ_z as would be expected from the release Richardson number.

Acknowledgements

The authors gratefully acknowledge the support of the U.S. Coast Guard Office of Research and Development, the Gas Research Institute, and the U.S.

Air Force Engineering and Services Center through Contract DTCG23-80-C-20029.

List of symbols

b	half width of horizontally homogeneous central section of gas plume (m)
c	concentration (kg/m^3)
c_c	centerline, ground-level concentration (kg/m^3)
C_E	constant in density intrusion (spreading) relation
D	source diameter
g	acceleration of gravity (m/s^2)
H	height or depth of density intrusion or cloud (m)
$(H/D)_i$	initial height-to-diameter (aspect) ratio
H_{EFF}	effective cloud depth (m)
H_i	initial cloud height (m)
K_c	vertical turbulent diffusivity, mass (m^2/s)
K_H	vertical turbulent diffusivity, heat (m^2/s)
K_M	vertical turbulent diffusivity, momentum (m^2/s)
k	von Karman's constant, 0.35
$\dot{m}$	mass source evolution rate (kg/s)
$(OBS/PRE)_y$	ratio of "observed" distance to DEGADIS-predicted distance for the y concentration level
$(\overline{OBS/PRE})_y$	average of $(OBS/PRE)_y$
O( )	on the order of . . .
Q	volumetric release rate (m^3/s)
Q_*	atmospheric takeup flux ($kg/m^2 s$)
R	gas source cloud radius (m)
R_p	primary source radius (m)
Ri_c	release Richardson number for continuous releases
Ri_*	Richardson number
S_y	horizontal concentration scaling parameter (m)
S_z	vertical concentration scaling parameter (m)
t	time (s)
T	cloud temperature (K)
u	average wind velocity (m/s)
u_e	horizontal or frontal entrainment velocity (m/s)
u_{EFF}	effective cloud advection velocity (m/s)
u_f	cloud front velocity (m/s)
u_x	wind velocity along x-direction (m/s)
u_0	wind velocity measured at $z=z_0$ (m/s)
u_*	friction velocity (m/s)
V_i	initial volume (m^3)

w_e'	entrainment velocity associated with H_{EFF} (m/s)
x,y,z	Cartesian coordinates (m)
y_v	contaminant mole fraction
z_0	reference height in wind velocity profile specification (m)
α	constant in power law wind profile
Δ'	ratio of $(\rho-\rho_a)/\rho_a$
ρ	density of gas-air mixture (kg/m^3)
ρ_a	ambient air density (kg/m^3)
ρ_i	initial cloud density (kg/m^3)
σ_y	Pasquill–Gifford lateral dispersion coefficient (m)
σ_z	Pasquill–Gifford vertical dispersion coefficient (m)

References

1 J.A. Fay and S.G. Zemba, Dispersion of initially compact dense clouds, Atmos. Environ., 19(8) (1985) 1257–1261.
2 R.G. Picknett, Dispersion of dense gas puffs released in the atmosphere at ground level, Atmos. Environ., 15 (1981) 509–525.
3 D.J. Hall, E.J. Hollis and H. Ishaq, A wind tunnel model of the Porton dense gas spill field trials, LR 394 (AP), Warren Spring Laboratory, Department of Industry, Stevenage, U.K., 1982.
4 R.N. Meroney and A. Lohmeyer, Gravity spreading and dispersion of dense gas clouds released suddenly into a turbulent boundary layer, Draft Report CER82-83RNM-AL-7 to Gas Research Institute, Chicago, IL, August 1982.
5 J.A. Havens and T.O. Spicer, Gravity spreading and air entrainment by heavy gases instantaneously released in a calm atmosphere, in: G. Ooms and H. Tennekes (Eds.), Proc. I.U.T.A.M. Symposium on Atmospheric Dispersion of Heavy Gases and Small Particles, Delft University of Technology, The Netherlands, August 29–September 2, 1983, Springer, Berlin, 1984.
6 T.O. Spicer and J.A. Havens, Modelling the phase I Thorney Island experiments, J. Hazardous Materials, 11 (1985) 237–260.
7 S.R. Hanna, G.A. Briggs and R.P. Hosker, Handbook on Atmospheric Dispersion, DOE/TC-11223, 1982.
8 F. Pasquill and F.B. Smith, Atmospheric Dispersion, Halstead Press, New York, 3rd edn., 1983.
9 J.S. Turner, Buoyancy Effects in Fluids, Cambridge University Press, Cambridge, U.K., 1973.
10 J. McQuaid, Some experiments on the structure of stably stratified shear flows, Technical Paper P21, Safety in Mines Research Establishment, Sheffield, U.K., 1976.
11 L.H. Kantha, O.M. Phillips and R.S. Azad, On turbulent entrainment at a stable density interface, J. Fluid Mech., 79 (1977) 753–768.
12 K. Lofquist, Flow and stress near an interface between stratified liquids, Phys. Fluids, 3(2) (1960) 158–175.
13 J.A. Businger, J.C. Wyngaard, Y. Izumi and E.F. Bradley, Flux-profile relationships in the atmospheric surface layer, J. Atmos. Sci., 28 (1971) 181–189.
14 J.A. Havens and T.O. Spicer, Development of an atmospheric dispersion model for heavier-than-air gas mixtures, U.S. Coast Guard Report CG-D-22-85, May 1985.

15 G.W. Colenbrander, A mathematical model for the transient behavior of dense vapor clouds, in: 3rd International Symposium on Loss Prevention and Safety Promotion in the Process Industries, Basel, Switzerland, 1980.
16 G.W. Colenbrander and J.S. Puttock, Dense gas dispersion behavior: experimental observations and model developments. In: Proc. International Symposium on Loss Prevention and Safety Promotion in the Process Industries, Harrogate, England, September 1983.
17 A.P. van Ulden, A new bulk model for dense gas dispersion: two-dimensional spread in still air, in: G. Ooms and H. Tennekes (Eds.), Proc. I.U.T.A.M. Symposium on Atmospheric Dispersion of Heavy Gases and Small Particles, Delft University of Technology, The Netherlands, August 29–September 2, 1983, Springer, Berlin, 1984.
18 T.O. Spicer and J.A. Havens, Development of vapor dispersion models for non neutrally buoyant gas mixtures — Analysis of USAF/N_2O_4 test data, USAF Engineering and Services Laboratory, Final Report, May 1986.
19 J.R. Welker, Vaporization, dispersion, and radiant fluxes from LPG spills, U.S. Department of Energy Report DOE/EV/07020-1, May 1982.
20 J. McQuaid, Objectives and design of the Phase I heavy gas dispersion trials, J. Hazardous Materials, 11 (1985) 1–34.
21 R.P. Koopman, J. Baker, R.T. Cederwall, H.C. Goldwire, Jr., W.J. Hogan, L.M. Kamppinen, R.D. Keifer, J.W. McClure, T.G. McRae, D.L. Morgan, L.K. Morris, M.W. Spann, Jr. and C.D. Lind, Burro Series Data Reports, LLNL/NWC 1980 LNG Spill Tests, Lawrence Livermore National Laboratories Report UCID-19075, December 1982.
22 G.W. Colenbrander, A.E. Evans and J.S. Puttock , Spill tests of LNG and refrigerated liquid propane on the sea, Maplin Sands, 1980: dispersion data digests, Shell Thornton Research Center, May 1984 (confidential).
23 T.G. McRae, Analysis and model/data comparisons of large-scale releases of nitrogen tetroxide, Lawrence Livermore National Laboratories Report UCID-20388, June 1985.
24 R.E. Britter, The ground level extent of a negatively buoyant plume in a turbulent boundary layer, Atmos. Environ., 14 (1980) 779–785.
25 A. Evans and J.S. Puttock, Experiments on the ignition of dense flammable gas clouds, in: Proc. International Symposium on Loss Prevention and Safety Promotion in the Process Industries, Cannes, France, September 1986.